Deprotection, tethering and activation of a one-legged metalloporphyrin on a chemically active metal surface: NEXAFS, synchrotron XPS and STM study of [SAc]P-Mn(III)Cl on Ag(100)

*Mark Turner, Owain P. H. Vaughan, Georgios Kyriakou, David J. Watson, Lukas J. Scherer, Anthoula C. Papageorgiou, Jeremy K. M. Sanders, Richard M. Lambert**

Department of Chemistry, University of Cambridge, Cambridge CB2 1EW, United Kingdom

RECEIVED DATE (to be automatically inserted after your manuscript is accepted if required according to the journal that you are submitting your paper to)

- Corresponding author. Email: rml1@cam.ac.uk; Tel.: +44 1223 336467; Fax: +44 1223 336362.

Abstract

The structural and reactive properties of the acetyl-protected “one-legged” manganese porphyrin [SAc]P-Mn(III)Cl on Ag(100) have been studied by NEXAFS, synchrotron XPS and STM. Spontaneous surface-mediated de-protection occurs at 300 K accompanied by spreading of the resulting thio-tethered porphyrin across the metal surface. Loss of the axial chlorine ligand occurs at 498 K, without any de-metallation of the macrocycle, leaving the Mn center in a low co-ordination state. At low coverages the macrocycle is markedly tilted towards the silver surface, as is the phenyl group that forms part of the tethering “leg”. In the monolayer region a striking transition occurs whereby the molecule rolls over, preserving the tilt angle of the phenyl group, strongly increasing that of the

macrocycle, decreasing the apparent height of the molecule and decreasing its footprint, thus enabling closer packing. These findings are in marked contrast with those previously reported for the corresponding more rigidly bound four-legged porphyrin [*JACS* **2009**, *126*, 1910] suggesting that the physico-chemical properties and potential applications of these versatile systems should be strongly dependent on the mode of tethering to the surface.

Introduction

Porphyrins tethered to solid surfaces have potential uses in a wide range of applications[1,2,3] including light-harvesting arrays,[4,5,6] optical switches and photonic wires.[2,3,7] Supramolecular arrays are of interest with respect to the study of energy transfer and photosynthetic mechanisms[7,8] while two-dimensional porphyrin assemblies have attracted attention for possible application as chemical sensors, in molecular electronics, or as chemically switchable 2D rotors.[3,9,10] Related to this, we recently showed that a porphyrin-functionalized silver surface exhibits ligand binding and unbinding reactions characteristic of the free metalloporphyrin[11] and showed that a well-chosen ligand can strongly alter the dynamics of adsorbed porphyrins.[10]

Porphyrins have been attached to oxide surfaces for use as sensors by means of organophosphonate linkers.[12] Our interest, however, lies in attaching metalloporphyrins to chemically active metal surfaces and we have reported a viable route for de-protecting and covalently attaching Mn porphyrin molecules to silver surfaces by means of *four* thio tethers.[13] The orientation, surface mobility and degrees of freedom of such covalently tethered porphyrins are expected to be important in determining access and escape of molecules to/from the porphyrin metal centre and hence their effectiveness in a variety of applications. One such application is catalysis, where Hulsken *et al.* have elegantly demonstrated that a Mn metalloporhyrin adsorbed on Au(111) catalyzed the aerobic epoxidation of stilbene in solution.[13] As extended Au surfaces cannot dissociatively adsorb oxygen,[15] a necessary precondition for epoxidation to occur,[16] the authors suggested that O_2 dissociation was a co-operative event involving two adjacent porphyrin molecules. Alternatively, by using a silver surface to dissociatively chemisorb dioxygen and deliver oxygen adatoms and a π-adsorbed alkene to the active metal centre of the porphyrin, one may

hope to create a hybrid, low temperature, selective oxidation catalyst. Accordingly, having investigated a rigidly tethered "four-legged" Mn porphyrin on Ag(100),[13] we report the properties of the corresponding acetyl-protected "one-legged" Mn porphyrin on the same surface. Substantial differences in mobility, spatial distribution, acetyl deprotection, dechlorination, flexibility and orientational behavior as a function of coverage are found indicating that the physico-chemical properties of porphyrin-functionalized surfaces should be markedly dependent on the mode of tethering. We also demonstrate that NEXAFS can be used to provide very detailed information about porphyrin adsorption geometry and changes in geometry with coverage, key properties in most applications.

In earlier studies, self-assembled porphyrin monolayers have been deposited on gold surfaces from solution.[14,18,19] Although these results are certainly interesting, the approach is not suited to our purpose—a SAM blankets the metal surface and excludes it from adsorbing reactants or participating in their further conversion to products. On the other hand deposition by vacuum evaporation allows close control of porphyrin coverage from submonolayers into the multilayer regime, making it the method of choice for our purposes. Often, porphyrin tilt angles have been inferred by considering factors such as packing density and surface periodicity without resort to direct spectroscopic measurements. Although infra red spectroscopy[20] does provide a reliable technique for determining porphyrin tilt angles, sensitivity is low, again precluding characterization of sub-monolayer coverages, which are the focus of our interest. So we have used near-edge X-ray absorption fine structure (NEXAFS) spectroscopy, high resolution synchrotron XPS and STM in conjunction with porphyrin deposition carried out under conditions of ultra high vacuum. NEXAFS provides extremely high sensitivity thus allowing investigation of sub-monolayer coverages, yielding orientational information about both the macrocycle and the attached phenyl group that forms part of the tethering leg: the ability to probe both N and C *K*-edge transitions is an added bonus.

Experimental Methods

The free base acetyl-protected porphyrin [SAc]P was synthesized following the procedure described by Ryppa *et al*.[21] Briefly, the acid-catalyzed condensation of dipyrromethane, pyrrole-2-carbaldehyde, and S-acetylthiobenzaldehyde in a "[2+1+1]" approach was used to produce two different *meso* substituted porphyrins: (i) [SAc]P porphyrin which has one substituent at position 5 (9.7 % yield) and (ii) $[SAc]_2P$ with two substituents at positions 5, 10 (11.4% yield). The two porphyrins were then separated by column chromatography. After crystallisation from dichloromethane : methanol, the compounds showed no detectable impurities. Metallation of the free-base porphyrin was achieved in a mixture of acetic acid : acetic anhydride = 4 : 1 at 110°C using $MnCl_2.4H_2O$ as the manganese source. After completion of the reaction the remaining inorganic salts were filtered off leaving the pure [SAc]P-Mn(III)Cl porphyrin (Figure 1).

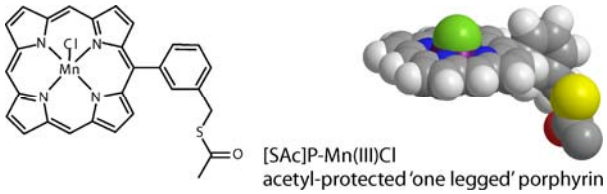

Figure 1. Molecular structure and 3D space-filling model for the 'one-legged' porphyrin, [SAc]P-Mn(III)Cl.

High resolution XPS and NEXAFS measurements were carried out on the SuperESCA beamline at the ELETTRA synchrotron radiation source in Trieste, Italy. Spectra were collected using a single-pass 32-channel concentric hemispherical electron analyzer. The excitation energies used for acquisition of the C 1s, Ag 3d, Cl 2p, S 2p, Mn 2p and N 1s spectra were 350 eV, 470 eV, 302.5 eV, 251 eV, 720 eV and 500 eV, respectively; the dwell time for signal averaging was 0.1 s. The angle between the analyzer entrance lens and the incoming photon beam was 70^o in the horizontal plane. The Ag(100) crystal was attached to a motorized manipulator *via* a tantalum backplate fitted with a T1T2 thermocouple and could be heated resistively to 900 K or cooled to 77 K. STM experiments were carried out in Cambridge, UK with an Omicron variable-temperature ultra high vacuum STM operated in constant

current mode using etched tungsten tips. The Ag(100) sample was cleaned by repeated cycles of Ar+ sputtering (99.999% Messer) followed by annealing at 600 K until a clean, atomically flat surface was obtained, as monitored by XPS and LEED (Trieste) or LEED, Auger electron spectroscopy and STM (Cambridge).

[SAc]P-Mn(III)Cl was deposited onto the Ag surface by means of a resistively heated collimated evaporation source fitted with a T1T2 thermocouple. The (very small) amounts of porphyrin used were injected into the sublimation source as solutions in dichloromethane which were then evaporated to dryness before mounting in the vacuum chamber. Calibration of the surface coverage was achieved by following the uptake of the porphyrin on Ag(100) using XPS[13] (Trieste) or estimated from STM images (Cambridge). Typically, porphyrin was deposited at room temperature followed by annealing at 473 K for 15 minutes to disperse initially formed islands and desorb any multilayer material. This method provided a convenient and reliable way of preparing any given coverage in the submonolayer to monolayer regime.[13]

Results and Discussion

Behavior at low coverage

Acetyl-protected [SAc]P-Mn(III)Cl was deposited on clean Ag(100) over 20 minutes, yielding an estimated sub-monolayer coverage of ~ 0.5 ML. Figure 2 shows N 1s XP spectra acquired (i) immediately after dosing and (ii) after annealing to 473 K for 15 min. In both cases only a single N 1s peak appeared – characteristic of a metallated porphyrin in which all N atoms in the macrocycle are equivalent. This is important because it confirms that no de-metallation occurred upon adsorption or heating: the free base porphyrin would exhibit two distinct N 1s signals corresponding to pyrrolic and iminic species.[22,23] The N 1s binding energies of these species are 400 eV and ~ 397 eV respectively so that they would have been readily resolved in our experiment. The weak Cl 2p emission and the undetectability of Mn 2p emission are consistent with the low number density of Cl and Mn atoms on the surface at saturation coverage, even though both were studied at the optimum photon energies that

maximized the respective photoionozation cross sections: Cl 2p = 3 Mb at 251 eV, Mn 2p = 1 Mb at 720 eV.[13] Both spectra in Figure 2 may be fitted with a single Gaussian centred at 397.2 eV (FWHM = 0.9 eV), assigned to Mn porphyrin molecules at sub-monolayer coverage. Annealing to 473 K caused no loss of N 1s intensity, confirming the absence of porphyrin multilayers. This behavior contrasts strongly with that of the corresponding four-legged Mn porphyrin which at 300 K form three-dimensional aggregates at low coverage, as observed by STM[24] and confirmed by XPS.[13] The implication is that in the present case reduced tethering results in increased mobility so that porphyrin spreading over the surface occurs even at room temperature.

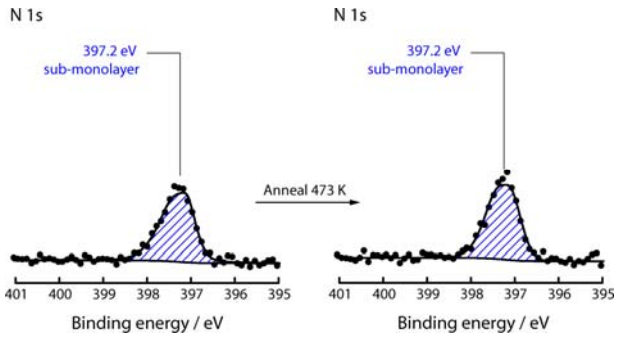

Figure 2. N 1s XP spectrum of a low (sub-monolayer) dose of one-legged porphyrin acquired before (left) and after annealing to 473 K (right) for 15 minutes.

The temperature dependence of the Cl 2p emission for the same porphyrin coverage is shown in Figure 3: the second and third spectra were obtained after annealing at 473 K and 498 K, respectively, for 15 minutes. It is clear that much of the axial chlorine ligand was lost during the first stage of annealing with no de-metallation having occurred (N 1s XPS unchanged) and by 498 K chorine loss was complete as a result of desorption,[13] perhaps accompanied by some dissolution[25] into the Ag, leaving the Mn center in a low-coordination state.[13] This behavior is somewhat different from that of the corresponding four-legged porphyrin ($[SAc]_4$P-Mn(III)Cl)[13] which was readily and completely dechlorinated on Ag(100) at 473 K.

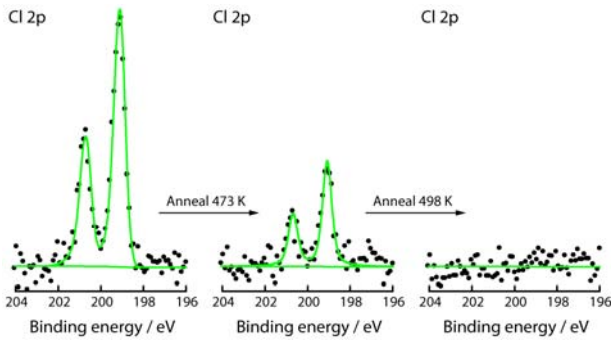

Figure 3. Cl 2p region of the XP spectrum of the one-legged porphyrin after initial dosing (left), after annealing to 473 K (center) and after annealing to 498 K (right).

N *K*-edge NEXAFS spectra acquired at five angles of photon incidence for the same low coverage (~ 0.5 ML) are shown in Figure 4(a). Clear resonances due to N 1s → π* and N 1s → σ* transitions are observed which display pronounced dependence on the photon incidence angle: peak assignments and associated transitions are presented in Table 1.[26,27,28]

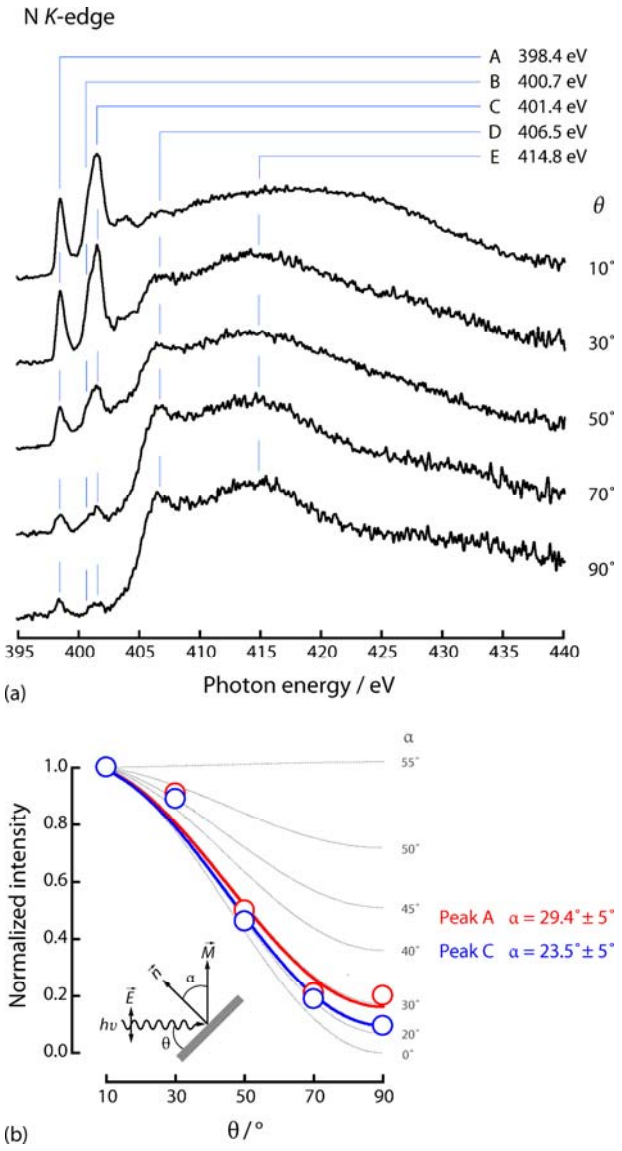

Figure 4. **(a)** N *K*-edge NEXAFS spectra acquired at five angles of photon incidence (*θ)* for a ~ 0.5 ML coverage of [SAc]P-Mn(III)Cl on Ag(100). **(b)** Curve fitting analysis of the photon angle dependence of π* resonances A and C to estimate the corresponding macrocycle tilt angle, α.

Table 1. Peak assignments for the N *K*-edge NEXAFS of [SAc]P-Mn(III)Cl on Ag(100)

Peak	Energy / eV	Assignment
A	398.4	N 1s → π*
B	400.7	N 1s → π*
C	401.4	N 1s → π*
D	406.5	N 1s → σ*
E	414.8	N 1s → σ*

The principal resonances **A** and **C** occur before the step edge and correspond to transitions from N 1s to each of the first two available π* orbitals, respectively. Resonance **B**, also due to a π* transition, appears as weak shoulder to **C**; two broad σ* resonances **D** and **E** occur beyond the step edge. A more detailed assignment of the final state orbitals and their symmetry would require comparison with simulated NEXAFS spectra[29] and is not necessary for our purposes. As expected, both π* and σ* resonances display distinct dichroism in their angular dependence. The absence of a strong resonance between **C** and **D** (at ~ 403 eV, characteristic of pyrrolic N in the metal-free base) confirms that the porphyrin is metallated and that the manganese metal centre is fully coordinated by the four central N atoms.

Since the N atoms reside within the center of the macrocycle and are approximately co-planar, the angular dependences observed in the N *K*-edge spectra provide a powerful means of determining the orientation of the metalloporphyrin with respect to the surface. Figure 4(b) presents such an analysis for the principal π* resonances **A** and **C**, the observed normalized intensities being overlaid with best-fit theoretical curves for the molecular tilt angle (α) with respect to the surface.[30] (In principle, σ* resonances may also be subjected to a similar analysis, but their width and superposition on the step background precludes accurate fitting.) A least-squares fit gives macrocycle tilt angles of 29.4° for **A** and 23.5° for **C**: the values are consistent within experimental error (+/-5°) and indicate that the porphyrin is very appreciably inclined with respect to the surface.

NEXAFS cannot distinguish between molecular tilt angles towards or away from the surface and Figure 5 shows the two possibilities corresponding to the present case. Of these, the second (**b**) is intuitively the more likely as it maximizes molecule-surface interaction. Taking account of the dimensions of the macrocycle and the tethering "leg", simple trigonometry confirms that a porphyrin *downward* tilt angle of 25° - 30° is possible (5.9 Å leg length, 11.0 Å macrocycle width, ~ 100° angle between leg and macrocycle). Moreover, STM data to be presented below are consistent with the downward tilt model.

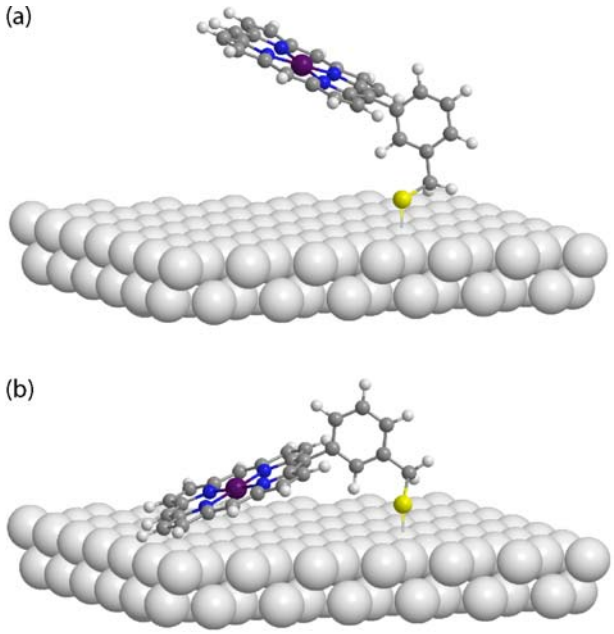

Figure 5. Two possible orientations of the one-legged porphyrin tethered to Ag(100) corresponding to the same macrocycle tilt angle of ~ 25° - 30°. **(a)** porphyrin tilted upwards and **(b)** porphyrin tilted downwards.

Figure 6 shows low coverage (~ 0.5 ML) C *K*-edge NEXAFS spectra acquired at five photon incidence angles. Five resonances are apparent, three C 1s → π* at lower photon energy and two C 1s → σ* at higher photon energy, beyond the step edge. (Table 2 lists peak assignments.) The improved s/n ratio compared to the N *K*-edge spectra reflects the ~ 7:1 C:N ratio in the molecule. Unlike the N *K*-edge spectrum, the C spectrum contains contributions from the phenyl substituent which forms part of

the tethering leg. In free porphyrins with phenyl substituents in the *meso* position, the latter are generally strongly tilted with respect to the central ring, so the angular dependence of the π* resonances is more complicated than in the N *K*-edge spectrum. In the past, this has led many groups to dismiss C *K*-edge spectra for the orientational analysis of phenyl-substituted porphyrins.[26] However careful inspection and assignment of each π* resonance does yield orientational information for *both* ring systems.[31,32]

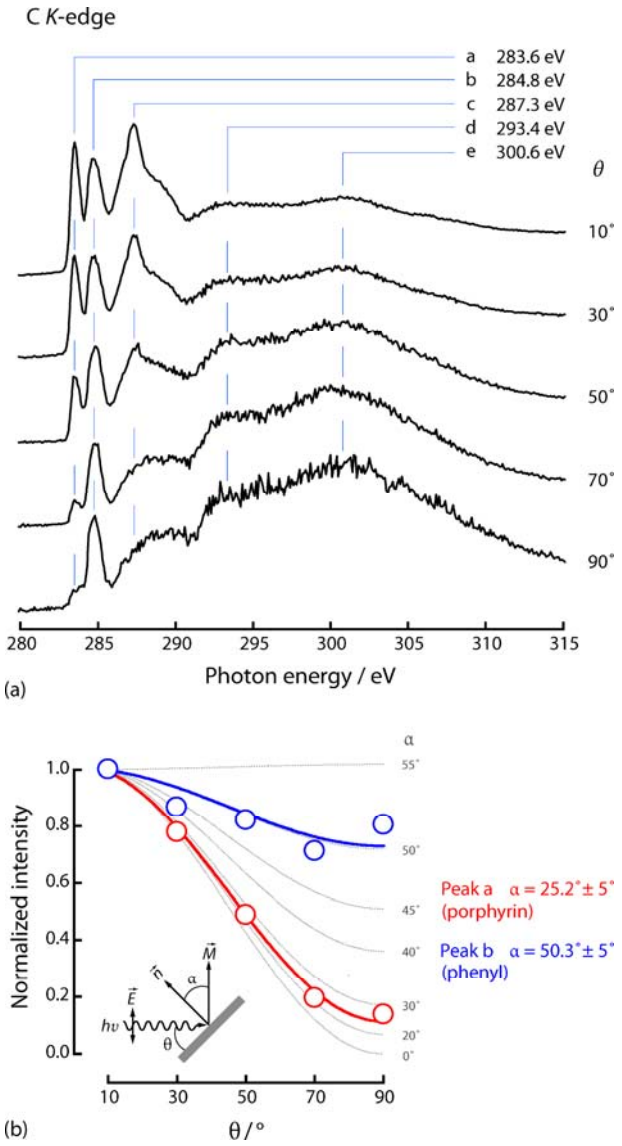

Figure 6. **(a)** C *K*-edge NEXAFS spectra acquired at five angles of photon incidence (*θ)* for a ~ 0.5 ML coverage of [SAc]P-Mn(III)Cl on Ag(100). **(b)** Curve fitting analysis of the photon angle dependence of π* resonances **a** and **b** to determine the corresponding macrocycle and phenyl tilt angles (α) respectively.

Table 2. Peak assignments for the C *K*-edge NEXAFS of [SAc]P-Mn(III)Cl on Ag(100).

Peak	Energy / eV	Assignment
a	283.6	C 1s → π* (porphyrin)
b	284.8	C 1s →π* (phenyl)
c	287.3	C 1s →π* (porphyrin)
d	293.4	C 1s →σ*
e	300.6	C 1s →σ*

Peaks **a** and **c** display the same type of angular dependence as the N spectrum π* resonances, and are assigned to C 1s → π* transitions involving the porphyrin ring. Peak **b** clearly exhibits a different angular dependence, the signal varying little with θ : it is therefore assigned to C 1s → π* transitions of the phenyl substituent. The results of a full analysis of the angular dependence of resonances **a** and **b** are shown in Figure 6(b). Resonance **a** corresponds to a porphyrin ring tilt angle of 25.2° – within experimental error fully consistent with the value derived from analysis of the N *K*-edge data. Resonance **b** yields a tilt angle of 50.3° for the phenyl ring – as expected, this indicates significant tilt of the phenyl ring with respect to the plane of the porphyrin ring. Taking account of the macrocycle tilt of ~ 30°, we conclude that the phenyl group lies at ~ 80° to the porphyrin plane – i.e. much as would be expected for the free molecule, and consistent with the illustration in Figure 5b.

STM imaging of 300 K as-deposited submonolayer coverages showed that no morphological changes occurred upon annealing to 473 K, in good accord with the corresponding N 1s XPS results, and typical images are shown in Figure 7. The lateral dimensions of individual features correspond to those expected for porphyrin molecules. Their apparent height of ~ 1.9 Å is comparable to the apparent height of ~ 2.3 Å recorded for the analogous 4-legged porphyrin on Ag(100)[24] — consistent with a downward tilted macrocyle ring in the present case. An upwardly tilted molecule would have an apparent height of about twice this value. Most molecules are characterized by a bright central spot which we associate with the Cl ligand attached to the Mn center, consistent with the Cl XP spectrum

shown in Figure 3, and in good accord with the line scans in Figure 7(c) for chlorinated and de-chlorinated molecules. Also visible are a number of smaller features (green circles Figures 7(a)) identified as acetyl groups[24] resulting from spontaneous surface mediated de-protection of the thiol group by cleavage of the acetyl group initially present at the end of the leg. The dimensions of these smaller features (~ 4.5 Å lateral, apparent height 0.65 Å) are commensurate with those of an acetyl group.[24] Figure 7(a) is a larger scale image of porphyrin molecules in the contact layer and the cleaved acetyl groups: examination of several images with a total area of 2760 nm^2 showed that the ratio of porphyrin molecules to cleaved acetyl groups was ~ 1:1.4 in reasonable accord with the expected value of 1:1. Thiol-deprotection was confirmed by the S 2p XP spectrum – a single S $2p_{3/2}$ component at a binding energy of 162.3 eV appeared, corresponding to deprotected molecules bound to the metal surface.[13]

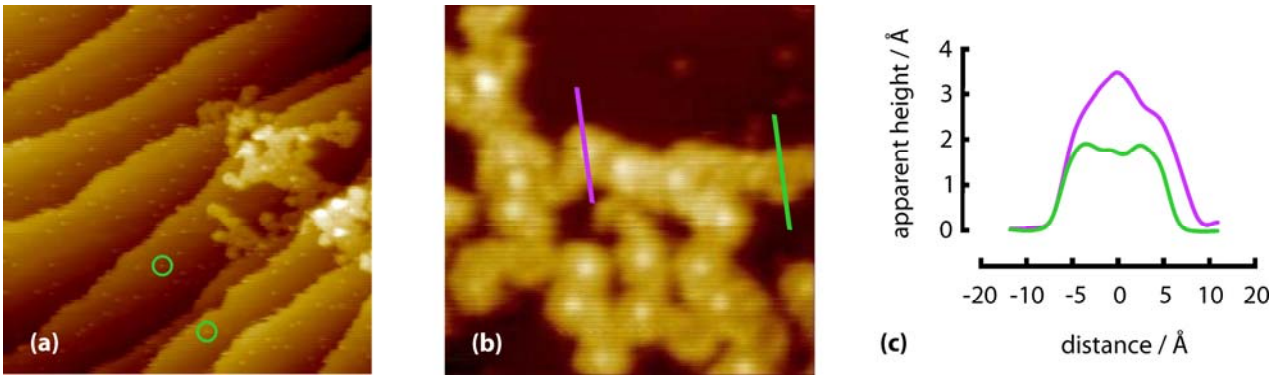

Figure 7. STM images and line profiles of a sub-monolayer coverage of the one-legged porphyrin acquired after annealing to 473K. (**a**) (360 x 360 $Å^2$, V_{tip}= 1.00 V, I = 1.02 nA). Two cleaved acetyl groups circled in green. (**b**) Small scale image showing positions of line scans taken through chlorinated and de-chlorinated molecules. (75 x 75 $Å^2$, V_{tip}= 1.00 V, I = 1.01 nA) (**c**) Line scans taken at the positions indicated in (b).

Behavior at high coverages

Behavior at higher coverages was investigated by depositing more porphyrin on top of the 300 K ~ 0.5 ML deposit and N 1s XP spectra taken before and after annealing to 473 K are shown in Figure 8.

Three components may be discerned in the 300 K as-deposited film: one centered at 397.2 eV corresponding to the low coverage N 1s spectrum (*cf* Figure 2); a principal component centered at 397.7 eV that we assign to a dense monolayer phase in contact with the Ag surface; and one at 398.5 assigned to molecules in a multilayer configuration. Annealing to 473 K resulted in the N 1s spectrum shown in the right panel of Figure 8. The multilayer component is strongly attenuated, the sub-monolayer contribution is absent, and molecules in the dense contact layer are the predominant species: heating has resulted in spreading of the initially inhomogeneous film. This observation is in good agreement with the STM image (Figure 9) acquired in Cambridge for a nominal porphyrin coverage of ~ 1.1 ML, (estimated by STM). Line scans through molecules in the dense contact layer indicate an apparent molecular height of 1.6 Å, which is smaller than that found for molecules in the low coverage regime (1.9 Å); as we shall see, this finding assists interpretation of the corresponding NEXAFS results.

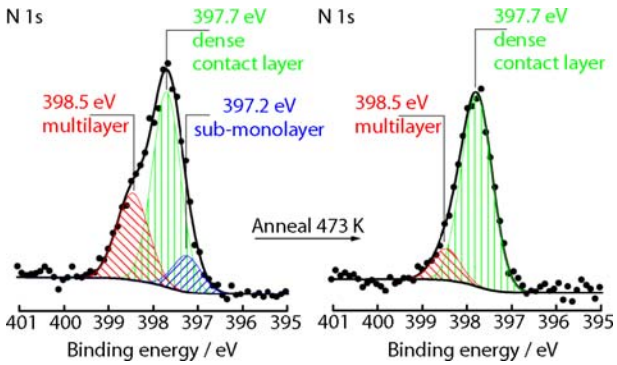

Figure 8. N 1s XP spectra for a high coverage of porphyrin as deposited (left) and after annealing to 473 K (right).

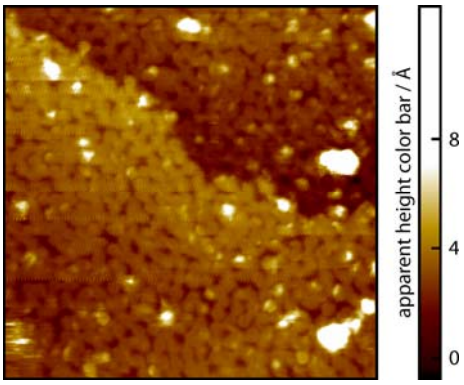

Figure 9. STM image (300 x 300 Å^2, V_{tip}= 1.21 V, I= 0.84 nA) of the densely packed contact layer of the one-legged porphyrin acquired after multilayer deposition and annealing to 473 K. White blobs are molecules in the second layer, as judged by apparent height.

N and C *K*-edge NEXAFS spectra acquired from the as-deposited high coverage film showed no energy shifts or changes in peak shape compared to the submonolayer spectra, indicating minimal changes in electronic structure with coverage. However, the high coverage spectra exhibit little dependence on photon incidence angle, indicating significant disorder in the inhomogeneous as-deposited porphyrin film (see supplementary information).

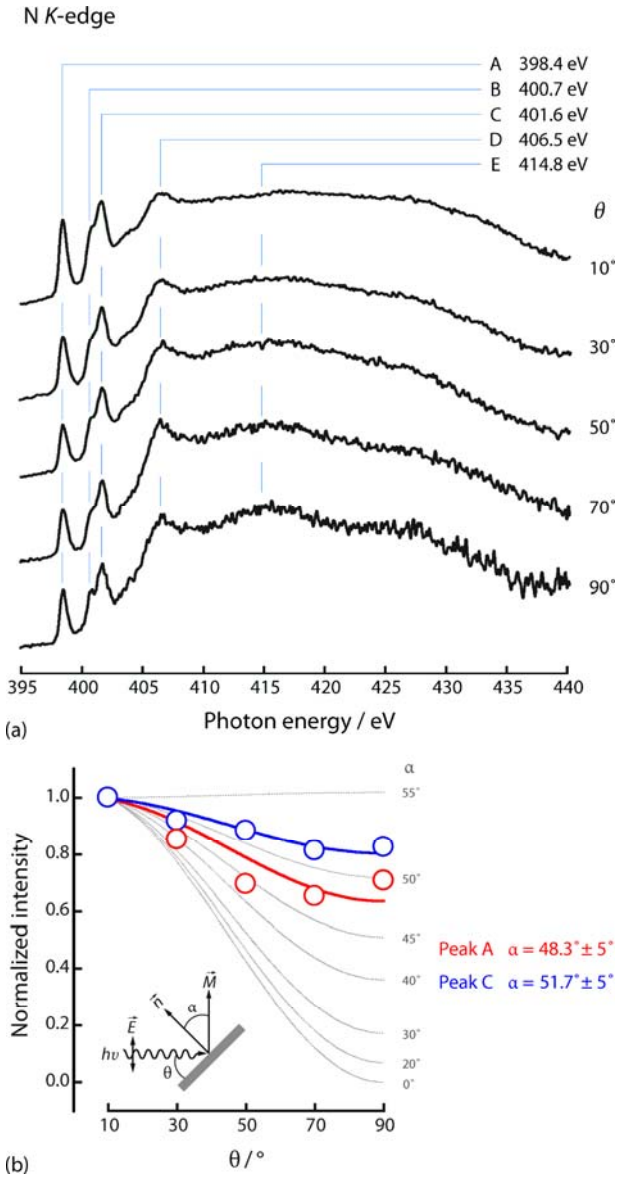

Figure 10. **(a)** N *K*-edge NEXAFS spectra acquired at five angles of photon incidence (*θ)* for a ~ 1 ML coverage of [SAc]P-Mn(III)Cl on Ag(100). **(b)** Curve fitting analysis of the θ dependence of π* resonances A and C to estimate the tilt angle (α) of the macrocycle.

After 473 K annealing both the N *K*-edge and C *K*-edge NEXAFS exhibited significant angular variation (Figures 10 and 11) consistent with removal of multilayer aggregates and smoothing of the contact layer, in line with both the XPS and STM results. XPS data taken before and after the acquisition of the NEXAFS spectra indicated no significant beam damage of the ~1 ML porphyrin film. Detailed analysis of the N *K*-edge resonances **A** and **C**, (Figure 10) yields estimated macrocycle tilt angles of ~ 48° and ~ 51°, respectively, *very substantially larger* than that found for the low coverage case (~ 29.4^{o} and ~ 23.5° respectively). Analysis of the corresponding C *K*-edge data for resonances **a** and **b** yields estimated tilt angles of ~ 51° and ~ 53° for the macrocycle and the phenyl group respectively, the markedly increased tilt derived for the former being in good agreement with the N edge results (Figure 10). In other words, at high coverage a transition occurs in the contact layer: compared to the low coverage case, the tilt of the phenyl group with respect to the surface remains unchanged whereas that of the macrocycle increases substantially. This change in adsorption geometry may be accounted for by allowing the molecule to roll over, as illustrated in Figure 12, preserving the tilt angle of the phenyl group, increasing that of the macrocycle, decreasing the apparent height of the molecule and at the same time *decreasing* its footprint, thus enabling closer packing. Note that the increased N 1s XPS binding energy relative to the low coverage value (397.7 eV *versus* 397.2 eV) may also be rationalized in terms of this change in adsorption geometry: at high coverage the nitrogen atom ends up further away from the surface resulting in decreased relaxation of the metal's valence electrons around the N core hole.

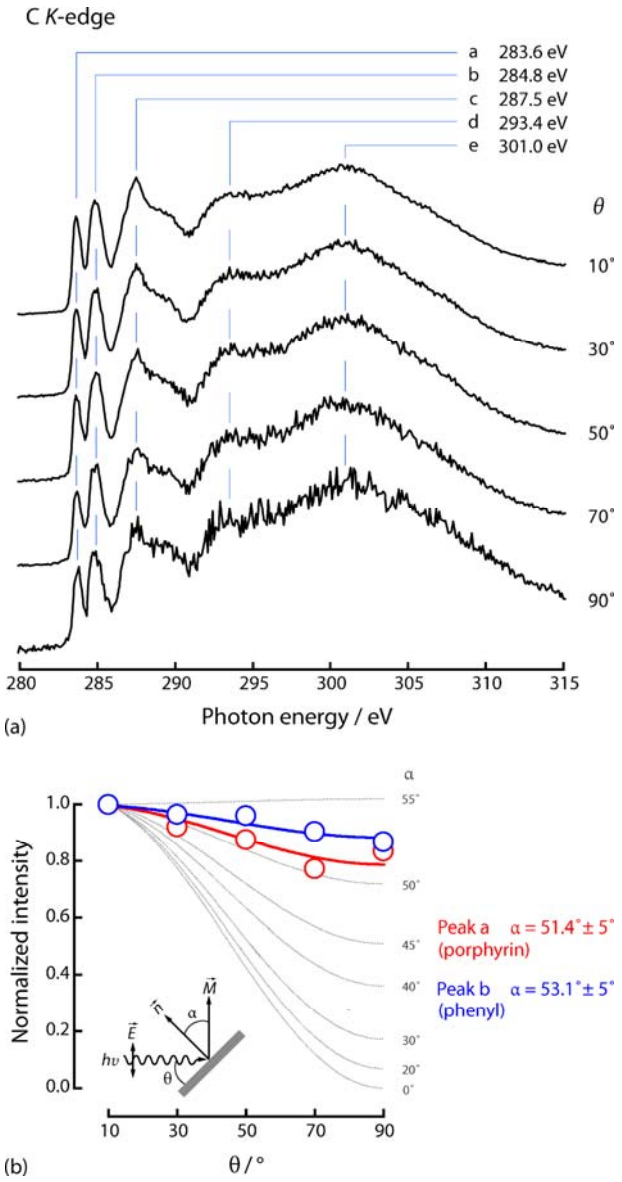

Figure 11. **(a)** C *K*-edge NEXAFS spectra acquired at five angles of photon incidence θ for a ~ 1 ML coverage of the one-legged porphyrin [SAc]P-Mn(III)Cl on Ag(100). **(b)** Curve fitting analysis of the angle dependence of π* resonances a and b to determine the corresponding π-system tilt angles α.

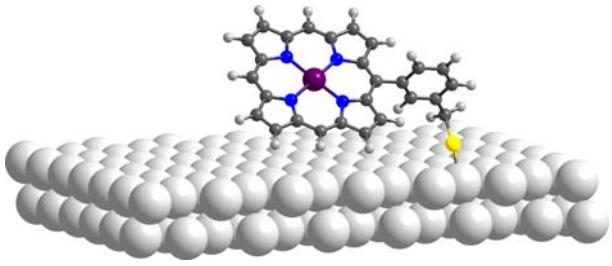

Figure 12. Proposed adsorption geometry of the one-legged porphyrin in the dense contact layer tethered to Ag(100). Macrocycle and phenyl tilt angles with respect to the surface are ~ 50° and ~ 53° respectively.

Conclusions

The one-legged acetyl-protected manganese porphyrin [SAc]P-Mn(III)Cl may be deposited without decomposition or de-metallation on Ag(100) and subsequently de-protected leading to covalently bound thio-porphyrin molecules. These in turn may be de-chlorinated, resulting in formation of stable, surface tethered low-coordinate Mn centers. At high coverage an unusual orientational transition occurs whereby the molecule rolls over, preserving the tilt angle of the phenyl group towards the surface, strongly increasing that of the macrocycle, decreasing the apparent height of the molecule and decreasing its footprint.

Compared to its more rigidly bound four-legged counterpart, the one-legged porphyrin exhibits substantial differences in mobility, spatial distribution, acetyl deprotection, dechlorination, flexibility and orientational behavior as a function of coverage. These properties are expected to be important in determining access and escape of molecules to/from the porphyrin metal centre and hence their effectiveness in a variety of applications. Thus the physico-chemical properties of porphyrin-functionalized surfaces should be markedly dependent on the mode of tethering of the macrocycle.

Acknowledgments

The authors are grateful to Silvano Lizzit, Sandra Gardonio and Michele Tranquilln for their assistance during the synchrotron experiments. M.T. and O.P.H.V. acknowledge financial support from Johnson Matthey plc and King's College, Cambridge, respectively. L.J.S. acknowledges financial support from the Swiss National Foundation and the Novartis Foundation. D.J.W, G.K and A.C.P. acknowledge financial support from the UK Engineering and Physical Sciences Research Council.

Supporting information available: N and C *K*-edge NEXAFS spectra acquired from the as-deposited high coverage porphyrin film. This material is available free of charge via the Internet at http://pubs.acs.org.

References

1. Drain, C. M.; Batteas, J. D.; Smeureanu, G.; Patel, S. *Dekker Encyclopedia of Nanoscience and Nanotechnology*; Taylor & Francis: New York, USA, 2004.
2. Kwok, K. S.; Ellenbogen, J. C. *Mater. Today* **2002**, *5*, 28.
3. Carroll, R. L.; Gorman, C. B. *Angew. Chem. Int. Ed.* **2002**, *41*, 4379.
4. Endo, M.; Fujitsuka, M.; Majima, T. *Chem. Eur. J.* **2007**, *13*, 8660.
5. Nakano, A.; Osuka, A.; Yamazaki, I.; Yamazaki, T.; Nishimura, Y. *Angew. Chem. Int. Ed.* **1998**, *37*, 3023.
6. Prathapan, S.; Johnson, T. E.; Lindsey, J. S. *J. Am. Chem. Soc.* **1993**, *115*, 7519.
7. Holten, D.; Bocian, D. F.; Lindsey, J. S. *Acc. Chem. Res.* **2002**, *35*, 57.
8. Kay, A.; Grätzel, M. *J. Phys. Chem.* **1993**, *97*, 6272.
9. Purrello, R.; Gurrieri, S.; Lauceri, R. *Coord. Chem. Rev.* **1999**, *190-192*, 683.
10. Vaughan, O. P. H.; Williams, F. J.; Bampos, N.; Lambert, R. M. *Angew. Chem. Int. Ed.* **2006**, *45*, 3779.
11. Williams, F. J.; Vaughan, O. P. H.; Knox, K. J.; Bampos, N.; Lambert, R. M. *Chem. Commun.* **2004**, 1688.

12. Dubey, M.; Bernasek, S. L.; Schwartz, J. *J. Am. Chem. Soc.* **2007**, *129*, 6980.

13. Turner, M.; Vaughan, O. P. H.; Kyriakou, G.; Watson, D. J.; Scherer, L. J.; Davidson, G. J. E.; Sanders, J. K. M.; Lambert R. M. *J. Am. Chem. Soc.* **2009**, *131*, 1910.

14. Hulsken, B.; Van Hameren, R.; Gerritsen, J. W.; Khoury, T.; Thordarson, P.; Crossley, M. J.; Rowan, A. E.; Nolte, R. J. M.; Elemans, J.; Speller, S. *Nat. Nanotechnol.* **2007**, *2*, 285.

15. Pireaux, J. J.; Chtaïb, M.; Delrue, J. P.; Thiry, P. A.; Liehr, M.; Caudano, R. *Surf. Sci.* **1984,** *141*, 211.

16. Grant, R. B.; Lambert, R. M. *J. Chem. Soc. Chem. Commun.* **1983**, 662.

17. Yasseri, A. A.; Syomin, D.; Malinovskii, V. L.; Loewe, R. S.; Lindsey, J. S.; Zaera, F.; Bocian, D. F. *J. Am. Chem. Soc.* **2004**, *126*, 11944.

18. Shimazu, K.; Takechi, M.; Fujii, H.; Suzuki, M.; Saiki, H.; Yoshimura, T.; Uosaki, K. *Thin Solid Films* **1996**, *273*, 250.

19. Zak, J.; Yuan, H.; Ho, M.; Woo, L. K.; Porter, M. D. *Langmuir* **1993**, *9*, 2772.

20. Wei, L.; Syomin, D.; Loewe, R. S.; Lindsey, J. S.; Zaera, F.; Bocian, D. F. *J. Phys. Chem. B* **2005**, *109*, 6323.

21. Ryppa, C.; Senge, M. O.; Hatscher, S. S.; Kleinpeter, E; Wacker, P.; Schilde, U.; Wiehe, A. *Chem. Eur. J.* **2005**, *11*, 3427.

22. Flechtner, K.; Kretschmann, A.; Bradshaw, L. R.; Walz, M.-M.; Steinrück, H.-P.; Gottfried, J. M. *J. Phys. Chem. C* **2007**, *111*, 5821.

23. Gottfried, J. M.; Flechtner, K.; Kretschmann, A.; Lukasczyk, T.; Steinrück, H.-P. *J. Am. Chem. Soc.* **2006**, *128*, 5644.

24. Vaughan, O. P. H.; Turner, M.; Williams, F. J.; Hille, A.; Sanders, J. K. M.; Lambert, R. M. *J. Am. Chem. Soc.* **2006**, *128*, 9578.

25. Goddard, P. J.; Lambert, R. M. *Surf. Sci.* **1977**, *67*, 180.

26. Narioka, S.; Ishii, H.; Ouchi, Y.; Yokoyama, T.; Ohta, T.; Seki, K., *J. Phys. Chem.* **1995**, *99*, 1332.

27. Okajima, T.; Yamamoto, Y.; Ouchi, Y.; Seki, K. *J. Electron. Spectrosc. Relat. Phenom.* **2001**, *114-116*, 849.

28. Wende, H.; Bernien, M.; Luo, J.; Sorg, C.; Ponpandian, N.; Kurde, J.; Miguel, J.; Piantek, M.; Xu, X.; Eckhold, Ph.; Kuch, W.; Baberschke, K.; Panchmatia, P. M.; Sanyal, B.; Oppeneer, P. M.; Eriksson, O. *Nat. Mater.* **2007**, *6*, 516.

29. Polzonetti, G.; Carravetta, V.; Iucci, G.; Ferri, A.; Paolucci, G.; Goldoni, A.; Parent, P.; Laffon, C.; Russo, M. V. *Chem. Phys.* **2004**, *296*, 87.

30. Stöhr, J.; Outka, D. A., *Phys. Rev. B* **1987**, *36*, 7891.

31. de Jong, M. P.; Friedlein, R.; Sorensen, S. L.; Öhrwall, G.; Osikowicz, W.; Tengsted, C.; Jönsson, S. K. M.; Fahlman, M.; Salaneck, W. R. *Phys. Rev. B* **2005**, *72*, 035448.

32. Li, N. Y.; Su, Z.; Coppens, P.; Landrum, J. *J. Am. Chem. Soc.* **1990**, *112*, 7294.

TOC GRAPHIC